Received March 3, 2019, accepted March 27, 2019, date of publication April 11, 2019, date of current version April 22, 2019.

Digital Object Identifier 10.1109/ACCESS.2019.2910254

4 × 4-Element Cavity Slot Antenna Differentially-Fed by Odd Mode Ridge Gap Waveguide

ABDULADEEM BELTAYIB[1], ISLAM AFIFI[1], (Graduate Student Member, IEEE), AND ABDEL-RAZIK SEBAK[1], (Life Fellow, IEEE)

Electrical and Computer Engineering Department, Concordia University, Montreal, QC H4B 1R6, Canada

Corresponding author: Abduladeem Beltayib (a_beltay@encs.concordia.ca)

ABSTRACT A differential feeding for a cavity slot antenna is presented. The proposed feeding is based on a simple mechanism rather than the traditional complex networks that suffer from high losses. It is based on exciting the first higher order mode (TE_{10}) of the ridge gap waveguide (RGW) by enlarging the ridge width. This enlargement would excite some undesired even modes that are suppressed by inserting a vertical perfectly electric conducting (PEC) wall in the middle of the waveguide based on the concept of magic tee operation. The proposed 4 ×4 cavity slot antenna is implemented using substrate integrated waveguide (SIW) technology. Two horizontal slots on the top of proposed wide RGW, representing the differential feeding approach, are implemented to feed the cavity slot antenna. The slots couple the fields with same amplitudes and 180° phase difference to the cavity. The electric fields of the two coupling slots have odd symmetry in the x-axis, and subsequently, uniform electric field distribution of the TE_{440} mode of a cavity can be excited. The 4/4 radiating slots are etched on the top of the cavity in a specific distribution to ensure having in-phase fields for broadside radiation with low-cross-polarization levels. The measurement and simulation results of the proposed cavity slot antenna are in a good agreement. The obtained results confirm that the proposed antenna achieves a relative bandwidth of 7.1% for −10-dB return loss, a gain of about 16.5 dBi, and a side lobe level about −17 dB in E-plane and −13.8 dB in H-plane. Moreover, the proposed antenna provides low cross-polarization levels (−35 dB in E-plane and −27 dB in H-plane) within the operating frequency band of 32.5 to 34.9 GHz. With this achieved low profile, high gain, and high efficiency of the proposed cavity slot antenna, it may have a great potential for millimeter-wave (MMW) applications.

INDEX TERMS Ridge gap waveguide, high order mode, differential feeding network, symmetric radiation, low cross polarization level, millimeter wave, back cavity antenna, substrate integrated waveguide.

I. INTRODUCTION

For future wireless networks, a high data rate is an essential requirement. Extensive researches have been carried out to take advantage of available spectrum resources. Most of the existing standards around the world operate in the range of 300 MHz–3GHz and that is expected to be depleted soon. For this reason, the current research's focus is to find an alternative, and millimeter-wave (MMW) band is the most suitable option in this regard [1]–[3]. Therefore, the MMW mobile broadband system has become the best candidate to provide the requirement of the fifth generation mobile communication system.

The associate editor coordinating the review of this manuscript and approving it for publication was Raghvendra Kumar Kumar Chaudhary.

Components and antennas design at millimeter-wave band is the primary phase for implementing mm-wave wireless communication systems. High gain with sufficiently large operating bandwidth, compact size and low losses are the essential requirements. Many previous research efforts are shown for realizing antennas and components work at MMW band based on different technologies (substrate integrated waveguide (SIW) [4], microstrip lines [5], non-radiative dielectric (NRD) waveguide [6], [7] and rectangular waveguide (RWG) [8], [9]).

Most of these developed technologies have some limitations that could adversely affect the performance of antennas or devices. Most of these technologies have a drawback of high dielectric losses and inability to handle high power, which is considered the most prominent threat in microwave

applications. In [8], [9], a coupler is designed based on rectangular waveguides (RWG). However, the rectangular waveguide is bulky and hard to be integrated with other devices at high frequencies in particular at millimeter wave (MMW) band.

SIW-based structures have the advantages of rectangular waveguides and planar configurations such as low loss compared with the microstrip and coplanar transmission lines, compact profile, and is easy to integrate with planar circuits. These features and benefits make SIW technology a promising nominee to be used in compact MMW antenna structures [10], [11]. A low-profile cavity-backed SIW slot antenna designed to enhance bandwidth by combining a two different eigenmodes is presented in [12]. However, this antenna's gain is less than 7 dB, which is relatively low for MMW application.

Correspondingly in [13]–[15], a single-fed low-cost high gain slotted cavity antenna based on SIW technology using high-order modes (TE_{330}, TE_{44}) are presented. However, building a single layer large array using probe-feed is hard to physically realize. Meanwhile, the designed single feed cannot provide equal power distribution on the slots especially at high order cavity modes. With unequal power distribution, the dominant mode will be weak, and this will affect the radiation pattern and the cross-polarization In addition, all these antennas have a disadvantage of narrow bandwidth which is about 5%.

In [16], [17], differential-fed patch antennas are used to achieve good performances such as low cross-polarization level and symmetry in E and H-plane radiation patterns. However, the network used for the differential feeding suffer from dielectric losses.

In this work, a slot cavity antenna fed by TE_{10}-mode RGW is presented. For achieving differential performance, a 4 × 4 cavity slot array is fed by using the proposed wide RGW, in which two slots are etched on the top plate of RGW. Because of this feeding technique, symmetrical radiation patterns with low cross-polarization level are achieved for the slot cavity antenna. Additionally, since RGW can be designed in printed form [18]–[21], the proposed wide RGW can be easily integrated with monolithic microwave integrated circuits. Up to the authors' knowledge, this proposed TE_{10}-mode RGW and its use as a differential feeding is presented for the first time in literature.

This paper is organized as follow. The structure of the unit cell of RGW, the configuration of proposed wide ridge mode, and their simulated results are presented and described in Section II. Section III shows how a magic tee is used to eliminate even modes while keeping only the odd mode. Finally, antenna configuration and results are presented in Section IV.

II. RIDGE GAP WAVEGUIDE ANALYSIS

A. UNIT CELL

The unit cell dimensions are chosen to have the operating band between 25GHz and 40GHz. The dispersion diagram of the unit cells is obtained using a commercial software (HFSS). The unit cell configuration is shown in Fig. 1(a), where the cells are molded by metallic cylinders with radius $b = 0.5$mm, height $d = 2.3$mm, period $a = 2.5$mm, and air gap height $h = 1$mm

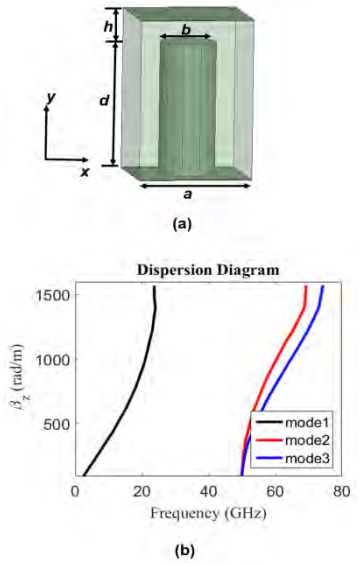

FIGURE 1. The configuration of unit cell and its dispersion diagram. (a) The configuration of the unit cell. (b) Dispersion diagram.

The dispersion diagram of the unit cell, shown in Fig. 1(b), is obtained based on assuming that the propagation is in the z-direction. From this dispersion diagram, it can be shown that there is a band gap from 22 GHz to 50 GHz.

B. RGW SECTION

In order to realize the complete RGW, a metal ridge with width w is used as shown in Fig. 2(a). The ridge width is chosen to be $w = 7.5$mm in order to guarantee the excitation of the fundamental (quasi-TEM) and the higher order modes (TE_{m0}) over the operating bandwidth. Using the Eigen mode solver in high frequency structure simulator (HFSS), the dispersion diagram of the RGW can be obtained as shown in Fig.2 (b). The RGW section consists of a ridge line surrounded by three bandgap unit cells from each side (Fig. 2 (a)). Periodic (master and slave) boundary condition is applied along the z-axis, while a periodic or PMC boundary conditions are applied in the y-z planes at both ends of the RGW section (this boundary condition does not affect the ridge line modes of our interest as they are far from the ridge line). Perfect electric boundary conditions have been applied to the top and bottom of the RGW section (x-z planes). In the bandgap region (from 25 to 43 GHz), the propagating modes along the ridge are: (1) the quasi-TEM mode (first even mode which dotted in blue line), and (2) the first odd mode TE_{10} (which dotted in red line), and (3) the second even mode TE_{20} (which dotted in black line. The other modes that appear on both sides of the bandgap region are out of our scope.

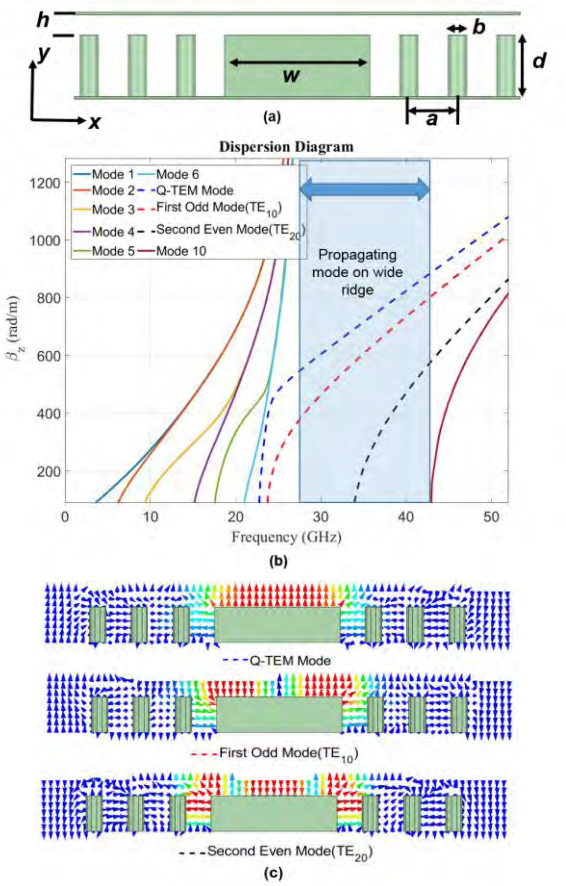

FIGURE 2. The configuration of wide RGW and dispersion curves of RGW obtained from HFSS. (a) The configuration of wide RGW. (b) Dispersion diagram. (c) Electric field distribution of the first three modes proposed wide RGW.

Using HFSS, electric fields distribution of the first three modes propagate on the ridge between 25GHz to 43 GHz can be obtained, as shown in Fig. 2(c). From this figure, it is clear that both of the fundamental mode and second higher order mode have even symmetry while the first higher mode has odd symmetry.

All the modes excited within this RGW are propagating along the z-direction. The periodic bed of nails acts as a

perfect magnetic conductor (PMC) which satisfies the boundary conditions of this RGW structure [22]–[23]. Based on the PMC boundary conditions, one can write the expression for the electric field component on the ridge of the structure in Fig. 2(a) as follow

$$E_y = \sum_{m=0,2,4}^{\infty} E_m \cos(k_{xm}x)\, e^{-jk_m z} + \sum_{m=1,3,5}^{\infty} E_m \sin(k_{xm}x)\, e^{-jk_{zm}z} \quad (1)$$

where $x = 0$ is taken at the center of the ridge.

The Electric field distribution for the TEM, TE10 and TE20 modes at the middle of the air gap along the x-axis can be approximated by the curves shown in Fig. 3 based on equation (1). From Fig. 3, it can be observed that the field distribution of the two even modes in RGW is maximum in the center and at the PMC walls ($w/2$) while the odd mode is maximum at the PMC walls and vanishes at the center.

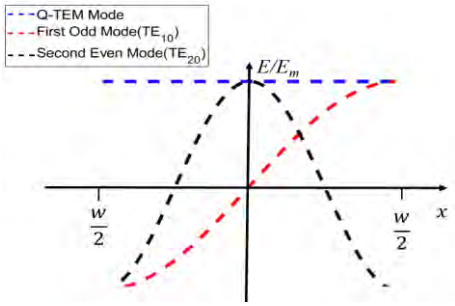

FIGURE 3. Cross sectional fields distribution of the first three modes.

The proposed cavity slot antenna is designed to be excited differentially by the RGW TE_{10} mode. Accordingly, both the quasi-TEM and the TE_{20} modes that shown in dispersion diagram should be suppressed to guarantee single mode operation. In view of Fig. 3, if a vertical PEC wall located on the origin point (0,0) on the graph, only fist odd mode (dotted red line) satisfy the boundary condition at the PEC wall while the other even modes (Q-TEM and second even modes) (dotted blue and black line respectively) do not satisfy the new boundary condition, where those modes have a maximum E-field at the center. Therefore, in such structure with such boundary conditions, only the odd mode will be propagated on the ridge. So by imposing a PEC wall at the middle of the ridge line, the even modes are eliminated and only the odd mode exist. To prove that, the following ridge gap waveguide with a PEC wall at the middle is investigated and the corresponding dispersion diagram is shown in Fig. 4(a). From the dispersion diagram shown in Fig. 4(b), it is clear that there is only one propagating mode TE_{10}, from 25 GHz to 43 GHz.

In order to verify this analysis, a simulated results of electric fields distribution of the propagated modes of RGW with PEC wall is shown in Fig. 4(c). From this figure, it is clear that only the odd mode (TE_{10}) satisfies the new boundary condition.

The simulated E-field distribution of the TE_{10} mode in such a RGW structure is shown in Fig. 5. From this figure, one can notice the odd symmetry of the electric field with respect to the x-axis can be used to create two horizontal slots to differently feed the cavity.

III. TE10 MODE TRANSITION STRUCTURE

A. MAGIC TEE IMPLEMENTION

A vertical PEC wall over the ridge is necessary for ensuring the suppression of the undesired even modes to guarantee the propagation of only TE_{10} mode over the bandwidth for single mode operation. This vertical PEC in the form shown in Fig. 4(a) is hard to physically construct. As an alternative solution, the magic tee structure shown in Fig. 6 can be used

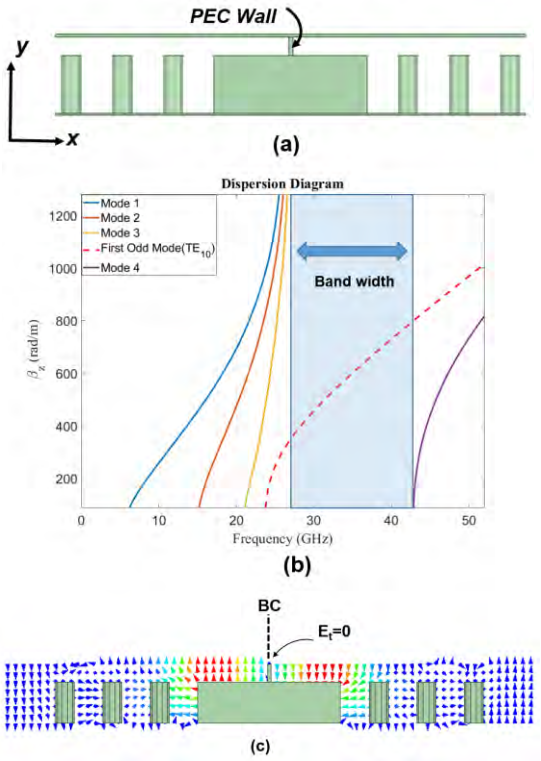

FIGURE 4. The configuration of RGW with PEC boundary at the middle and its dispersion curves. (a) The configuration of RGW. (b) Dispersion diagram. (c) Electric field distribution of the RGW.

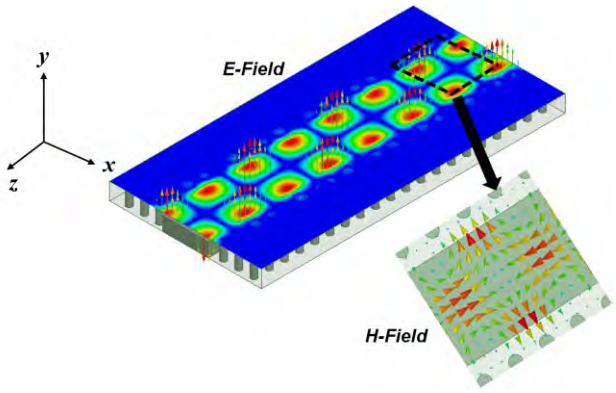

FIGURE 5. Electric and magnetic field distribution of the RGW first odd mode TE_{10} (proposed wide RGW).

to achieve the same behavior, but with a realizable geometry. The magic tee provides a differential excitation to the ridge line which imposes a virtual PEC wall at the middle of the ridge. Therefore, only the odd mode is excited on the ridge and the even modes are suppressed. A magic tee is commonly used to feed microwave systems. A traditional magic tee consists of four ports and can be used as an E-plane or H-plane power dividers. For example, when the power is applied to the difference port of the magic tee, the power will be equally divided between two ports with 180° phase shift and the remaining port is isolated. In this work, a short

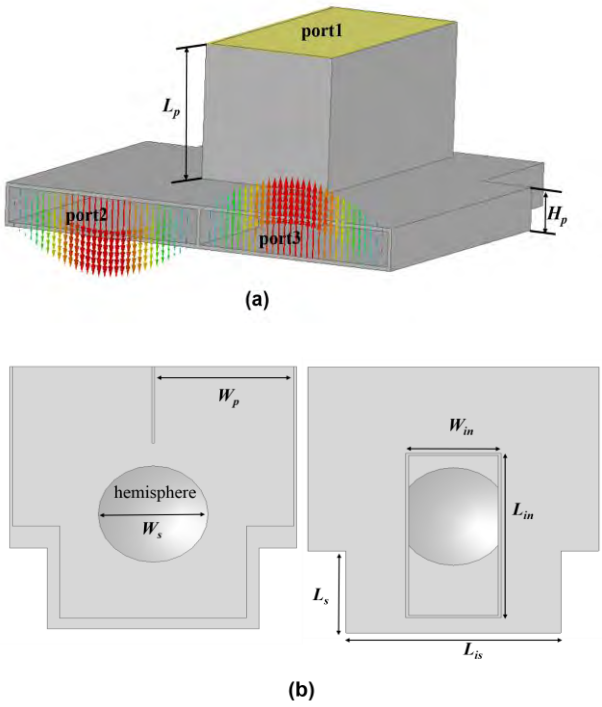

FIGURE 6. The configuration of the magic tee transition. (a) 3D view with the electric field distribution. (b) Top view right, middle cut left.

circuit is placed in the isolation port of the magic tee as it does not affect the magic tee performance. Fig. 6 (a) shows a 3D view of the three-port magic tee structure with all associated dimensions are listed in Table 1. In the shown geometry, port 1 is the input port while port 2 and port 3 are the output ports. When exciting this structure at port 1, the power is equally divided between port 2 and port 3 with 180° phase shift between them as clearly appears in the field distribution of Fig. 6(a). A hemisphere is used as shown in Fig. 6(b) in order to improve the matching [24].

TABLE 1. Dimensions of the magic tee.

parameter	W_{in}	L_{in}	W_p	H_p	W_s	L_s	L_{is}	L_P
Value(mm)	7.212	3.556	5.5	0.9	4.4	3.7	5.5	3.4

The simulated magnitude and phase responses of the S-parameters of the designed magic tee are shown in Fig. 7(a) and (b), respectively where the transmission levels to port 2 and port 3 are about −3 dB from 26 to 40 GHz, the reflection level at port 1 is below −20dB and the phase difference between port 2 and port 3 is 180 degrees.

B. RGW EXCITATION BY MAGIC TEE

In order to excite the proposed wide RGW, the magic tee shown in Fig. 6 is used where its output ports 2 and 3 are the inputs to the wide RGW as shown in Fig. 8(a), the top metal plate is hidden to show the inside structure. By applying the power to port1 of the magic tee, the power is equally

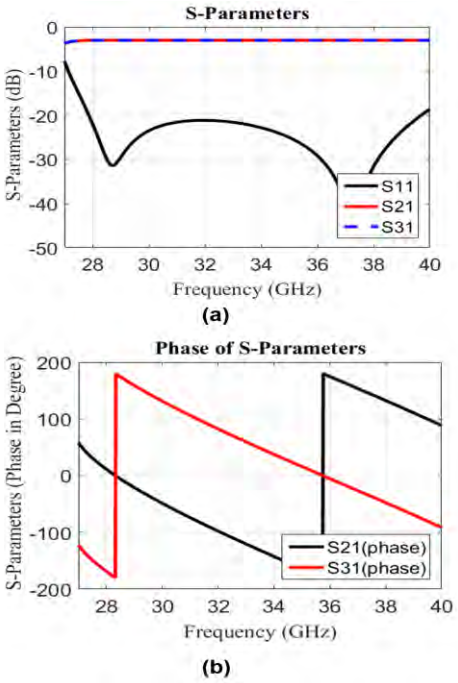

FIGURE 7. The magic tee S-parameters. (a) Magnitude. (b) Phase.

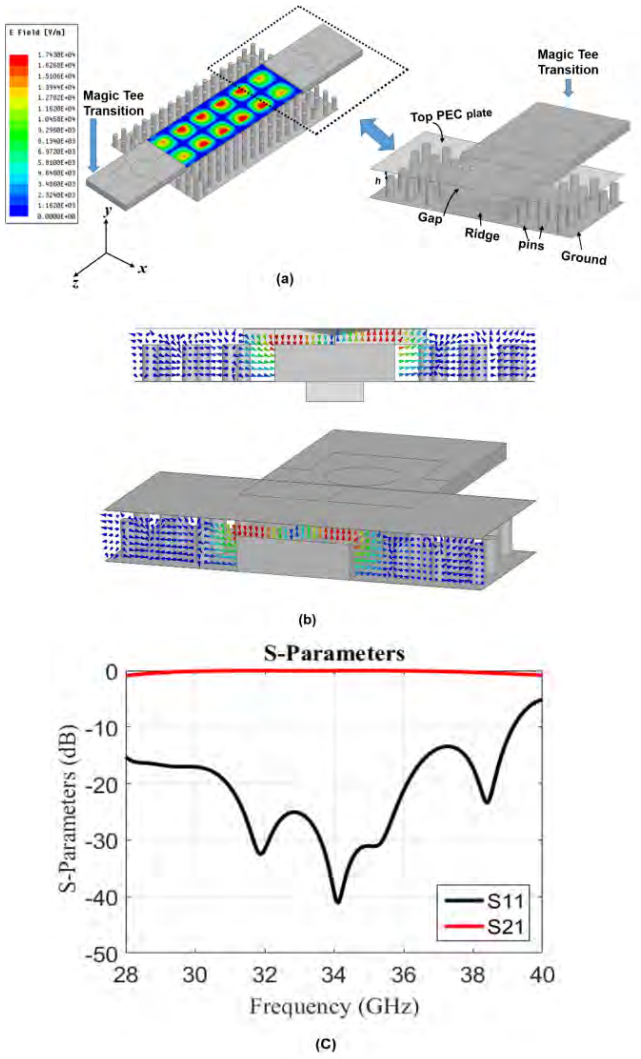

FIGURE 8. RGW with the magic tee transition. (a) Electric field distribution of the TE_{10} mode in the proposed RGW. (b) Electric fields distribution of a cross section of the magic tee of RGW. (c) S-parameters of back to back transition.

divided between port 2 and port 3 with 180° phase shift. Then those outputs are used as inputs of the proposed wide RGW. Fig. 8(b) shows the electric field distribution of the mode that can propagate in this ridge from different views. From the E-filed distribution, it is clear that there is only one propagating mode TE_{10} within the ridge with the tangential electric field is zero in the middle of the ridge and maximum on its sides.

By applying the superposition method of these two inputs, the even modes are eliminated while only the odd mode propagates inside the wide RGW. The simulated E-field distribution in RGW with the magic tee transition is shown also in Fig. 8(a). A very good matching is achieved over the whole bandwidth between 28 GHz and 39 GHz which is shown in Fig. 8(c).

IV. ANTENNA DESIGN

A. CONCEPT

Fig. 9 shows the H-field and E-field distribution inside a square waveguide cavity which is fed using two horizontal slots. From Fig.9 (a), it is clear that, there are 4 × 4 standing waves uniformly distributed in the cavity which demonstrates that the excited mode is TE_{440}. Thus, it is possible to excite this mode by using two horizontal slots as differential feeding in both sides of cavity center as shown in Fig. 9(b) (dotted black slot).

B. 4 × 4 CAVITY SLOT ANTENNA WITH DIFFERENTIAL RGW FEEDING

The configuration of the proposed cavity antenna and its feeding structure are shown in Fig. 10. A substrate integrated waveguide (SIW) cavity antenna is designed and excited by the RGW odd mode as a differential feeding technique to excite the TE440 mode inside the cavity. This cavity antenna is designed using Rogers 5880 ($\varepsilon r = 2.2$, $\tan\sigma = 0.002$) substrate with a thickness $hc = 1.58$mm. As shown in Fig. 10 (a), walls built by metallic vias are used to form the square cavity.

Based on the fields distribution inside the cavity, sixteen slots can be etched in phase on the top of the cavity as shown in Fig. 10 (a) where 4 × 4 standing waves are uniformly distributed in the cavity. As shown in Fig. 9(b), the slots distribute with equal shift distance ($S_c = 1.4$mm) from the dotted line. The electric field across the slots is shown in Fig. 9(b), where the black arrows describe the orientation of the electric field. Since all the slots are etched in phase, all the sixteen slots of the antenna radiate in phase. The cavity

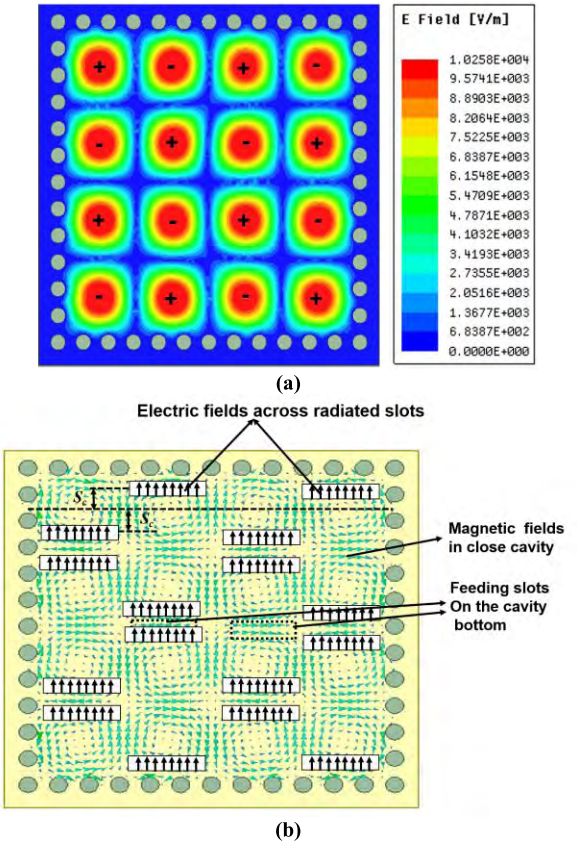

FIGURE 9. Magnetic and electric fields distribution of TE440 mode in square waveguide cavity. (a) The electric field in square waveguide cavity. (b) The magnetic field in the cavity and Electric field across the slots.

TABLE 2. Dimensions of proposed antenna.

parameter	W_{ridge}	L_{slot}	W_{slot}	D_{via}	h_c	P_{via}
Value(mm)	7.5	3.3	1.1	1	1.58	1.7
parameter	$Wc=L_c$	l_{match}	W_s	L_s	D_M	H_{short}
Value(mm)	19.8	2.5	0.6	4.4	0.27	1

antenna is excited by the structure shown in Fig. 10(b). All the dimensions of the proposed structure are listed in Table 2.

The integrated structure of 4 × 4 cavity slot antenna is shown in Fig. 10(c). The input field propagates along the wide RGW structure and couples to the cavity through the two horizontal slots that are etched on top of the RGW. Two vias with a radius of D_M and a height of H_{short} are positioned at the centers of the two coupling slots of the RGW. The vias, which are symmetric with respect to the z-axis, are built to improve the impedance matching.

The simulated results of the reflection coefficient and gain of the proposed cavity antenna are obtained using two full-wave solvers, namely the HFSS and the computer simulator technology (CST). The two independent solvers offer a considerable validation of the proposed design (HFSS uses finite element method while CST uses finite integral time domain method). The purpose from this comparison

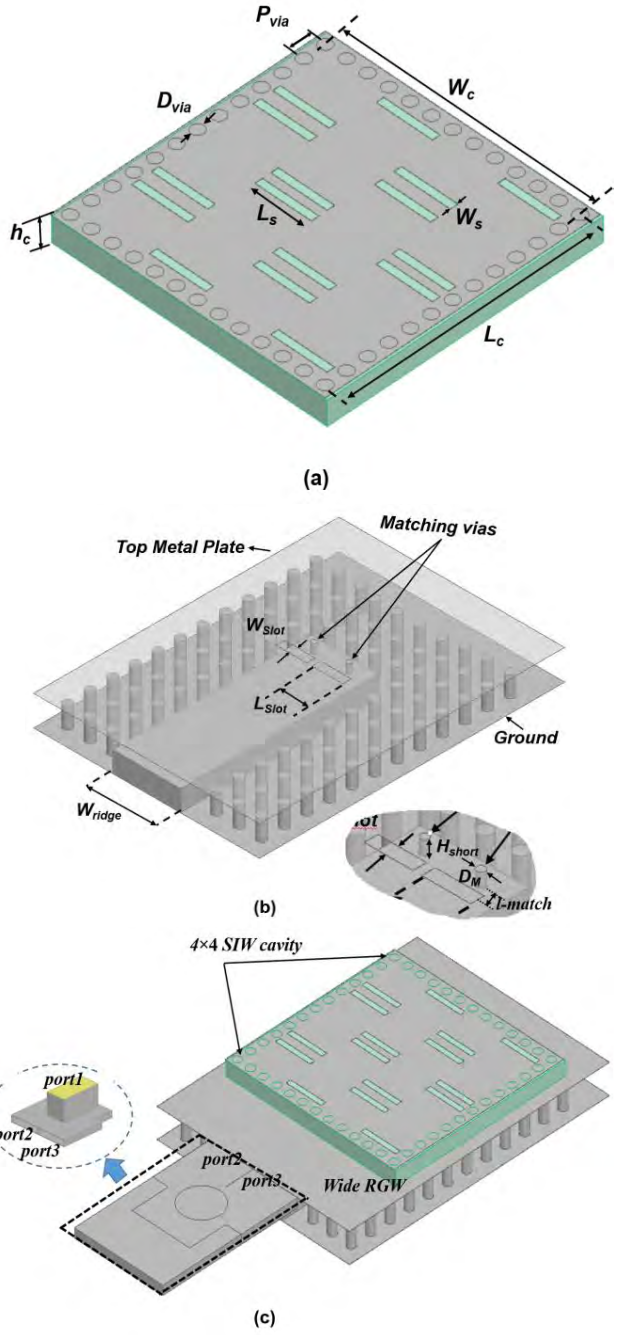

FIGURE 10. The geometry of the proposed cavity antenna structure. (a) 3D view of the SIW cavity. (b) Cavity excitation structure. (c) Whole cavity slot antenna structure.

is to provide a solid verification of the results before the fabrication stage.

As shown in Fig. 11, a very good agreement between the results is achieved. The fractional bandwidth is about 7.1% with a center frequency 33.5 GHz. The simulated gain is about 16.5 dBi over the bandwidth. It should be noted that one can use the same proposed feeding approach for feeding similar cavities made from different substrates such

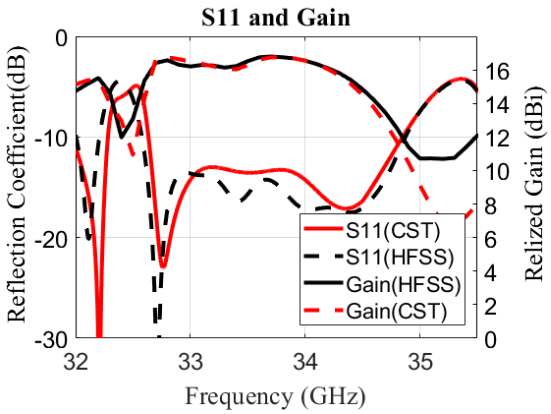

FIGURE 11. Comparison of the HFSS and CST simulated reflection coefficients and gains of the proposed cavity antenna.

as Rogers RT6002, Rogers RT5880 and Rogers RO3035,and can provide good performance.

V. PARAMETRIC STUDY

A parametric study has been carried out in order to show the effect of the most crucial dimensions on the proposed antenna performance, in terms of the gain and the reflection coefficient. The length of slot that etched on the top plate of RGW to feed the cavity (*L-slot*), matching pin position (*l-match*), substrate thickness (h_c), and cavity slot length and slot center offset (L_s and S_c) are selected for this parametric study.

The parametric study can be concluded in followed points:

- The matching pin position (*l-match*) and the length of the feeding slot (*l-slot)* have the same effect on the antenna's gain and matching performances, where increasing any one of them improves the gain and the matching until it reaches the optimum value. Then, the performance degrades again when moving away from the optimum value. This is illustrated in Fig. 12 where the gain and reflection coefficient with different values of the *l-match and l-slot* are presented. The optimum value of *l-match* and *l-slot* are 2.5mm and 3.3 mm respectively. The gain drops more than 1.5 dBi when moving away from the optimum values.
- The parametric study carry outed on cavity parameters h_c, and*ls*), shows a shift on the resonance frequency toward the lower frequencies when increasing any of them. This is depicted in Fig. 13(a), (c) where the gain and reflection coefficient for different values of h_c and *ls* is presented. The optimum values of*hc* and *ls* are 1.58mm and 4.4mm respectively. Also, there is a gain drop and degradation on the matching away from the optimum values.
- Changing *Sc* has a slight effect on the peak gain and the reflection coefficient. There is a drop in the gain at high frequencies for high values of *Sc* where the slots reaches the edge of the cavity. The optimum value of *Sc* is 1.4mm.

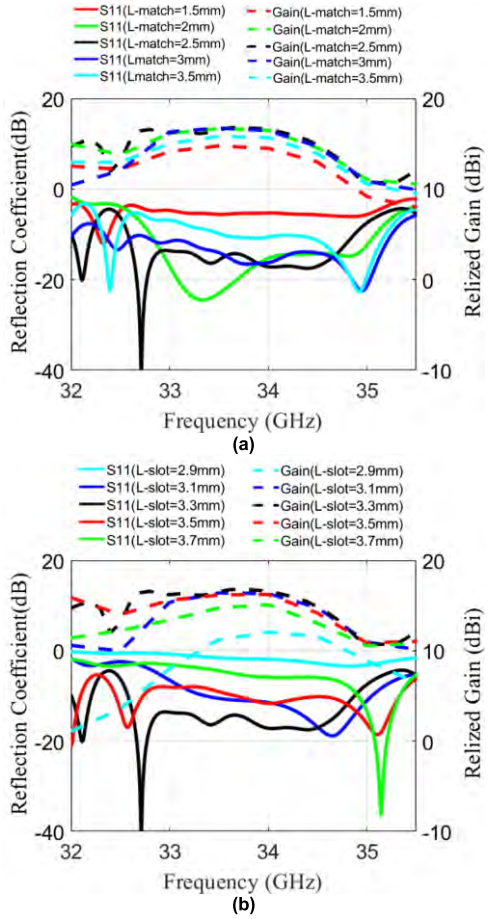

FIGURE 12. Simulated reflection coefficients and gain of the proposed antenna considering the impact of varying different geometric parameters of cavity feeding: (a) l-match; (b) L-slot.

VI. 3D PRINTING IMPLEMENTATION

In order to verify the proposed design, a prototype of the cavity slot antenna with differential feeding is fabricated as showed in Fig. 14(a,b). The feeding, the cavity antenna, and the transition are fabricated individually, then they are combined together by screws. The standard WR-28 waveguide is used to excite the structure at the Ka band. The technology used for the implementation of this structure is the three-dimensional printing of a plastic material, then the structure is plated with copper.

In the measurement setup, the antenna is mounted on fixture as illustrated in Fig. 15. The reflection coefficient of the antenna is measured by the Agilent N52271A network analyzer while the antenna radiation pattern and gain are measured in the antenna anechoic chamber by NSI far-field measurement system.

A. GAIN AND REFLECTION COEFFICIENT

The simulated and measured results of the reflection coefficient and gain of the proposed antenna are compared to each other as shown in Fig. 16. There is a good agreement between simulation and measurement results. The measured

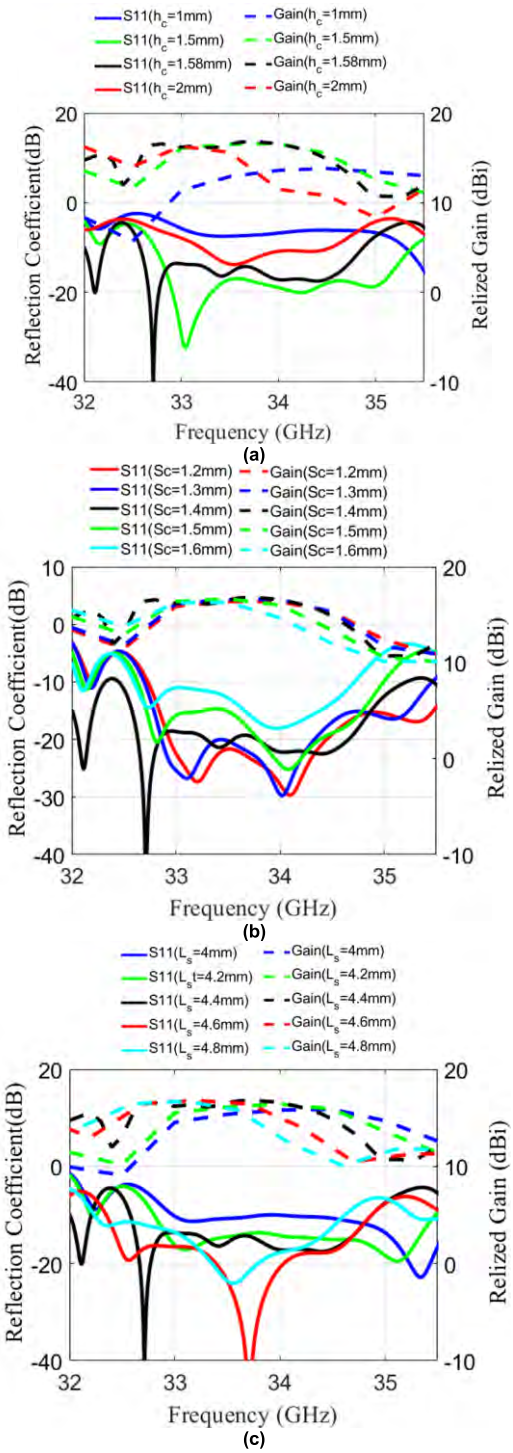

FIGURE 13. Simulated reflection coefficients and gain of the proposed antenna considering the impact of varying different geometric parameters of the cavity: (a) hc, (b) Ls, and (c) Sc.

fractional bandwidth of the structure is 8.3% (from 32.5 GHz to 35.3 GHz).The measured and simulated gains of the proposed antenna are also shown in Fig. 16 where both of them are around 16.5 dBi in the operating bandwidth. The slight difference between the simulated and measured results are due to the effect of the manufacture accuracy.

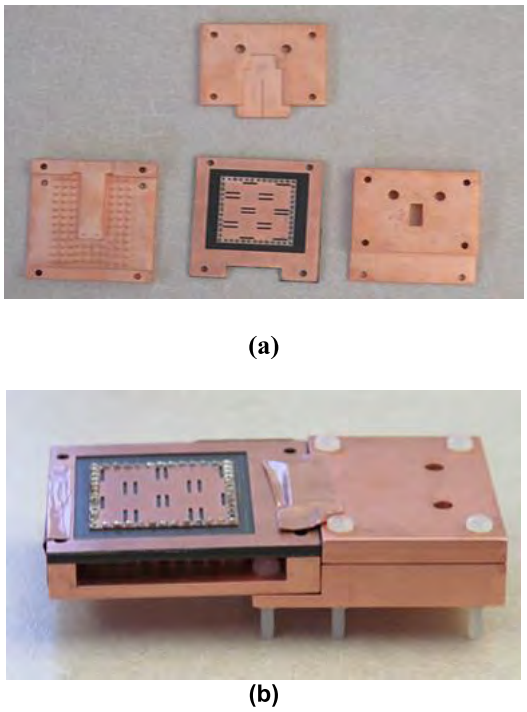

FIGURE 14. The fabricated 4 × 4 cavity antenna: (a) individual parts and (b) assembled parts.

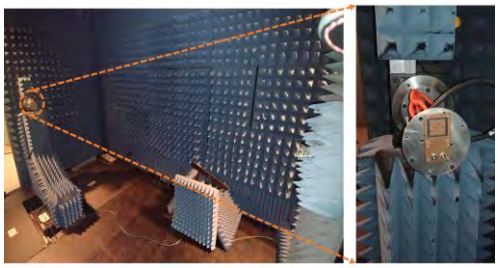

FIGURE 15. Photos of the measurement set up.

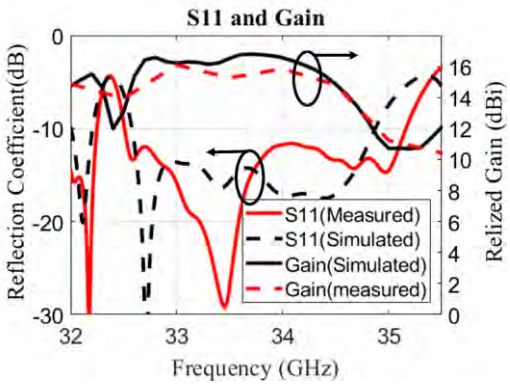

FIGURE 16. Comparison of simulated and measured reflection coefficients and gains of the proposed cavity antenna.

B. RADIATION PATTREN

The measured and simulated E-plane and H-plane radiation patterns of the proposed cavity antenna are illustrated in Fig. 17. The results are in a good agreement in both of E- and H-planes. The side lobe levels of E-plane and H-plane

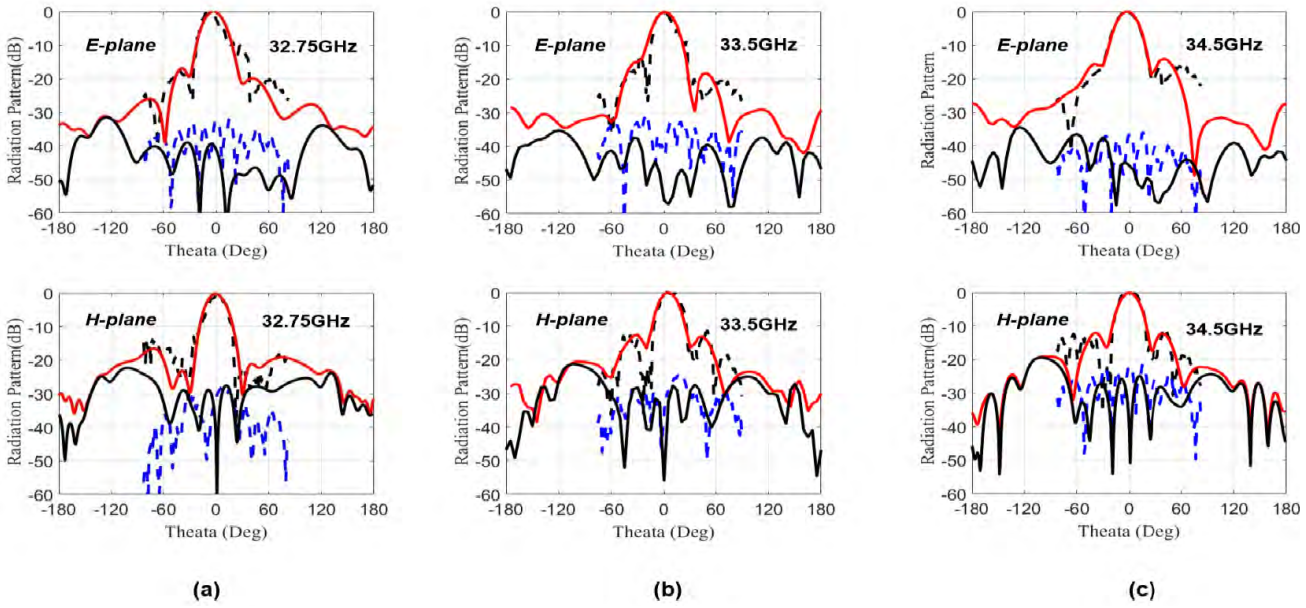

FIGURE 17. Measured and Simulated radiation patterns of the proposed cavity antenna. (a) 32.75 GHz. (b) 33.5 GHz. (c) 34.5 GHz.

TABLE 3. Comparison with previously antenna arrays.

Ref	Freq GHz	Feeding Type	Size (λ_0)	Elements	Gain (dBi)	BW (-10dB)	Aperture Efficiency	X-pol Level E and H plane
Ref[13]	5.8	Coaxial probe	1.6 λ_0 × 1.6 λ_0 × 0.029 λ_0	3 × 3	13.6	4.7%	71%	N.A
Ref[14]	28	Coaxial probe	2.16 λ_0 ×2.16 λ_0 ×0.17 λ_0	4 × 4	16	4.6%	83%	-23dB
Ref[15]	5.8	Coaxial probe	2.1 λ_0 ×2.1 λ_0 ×0.125 λ_0	4 × 4	15.2	3.4%	43%	-24dB
Ref[25]	35.25	SIW	5.83 λ_0 × 5.83 λ_0 ×0.18 λ_0	8 × 8	24.4	2.8%	65%	-30dB
Ref[26]	60	SIW	6.8 λ_0 × 4.95 λ_0 × 0.17 λ_0	6 × 8	21.6	1.8%	34.2%	-20
Ref[27]	35	SIW	4 λ_0 × 4 λ_0 × 0.3 λ_0	8×8	19.98	5.1%	47%	N.A
Ref[28]	10	SIW	1.03 λ_0 × 1.01 λ_0 ×0.05 λ_0	2×2	9.6	5.5%	69.8%	N.A
This work	33.5	TE10-mode RGW	2.22 λ_0 ×2.22 λ_0 × 0.17 λ_0	4 × 4	16.5	7.1%	72.8%	-35 dB and -27dB

patterns at 33.5 GHz are −17dB and −13.8dB, respectively. Since the cavity has symmetric shape and excited by differential feeding, the radiation patterns of the cavity are mainly symmetric especially in H-plane. The results show that the cross- polarization level is below −35 dB and −27 dB in the E-plane and H-plane, respectively, across the whole the operating bandwidth.

A comparison among related reported antennas and this work is listed in Table 3. Using the second order mode as a differential feeding for the cavity slot antenna presented in this work has some advantages compared to other antennas listed in the table. The proposed antenna has a superior radiation performance which has low cross polarization level, relatively higher gain, low side lobe level, symmetrical radiation pattern, and good aperture efficiency. Moreover, the matching bandwidth has been enhanced compared to the reported works.

VII. CONCLUSION

In this work, a differential excitation mechanism for a 4 × 4-element cavity slot array antenna is introduced and implemented using the TE_{10} mode of a wide RGW. The RGW

technology has been used in order to decrease the dielectric and radiation losses that can be caused by using other technologies especially at high frequency band as the wave propagates in an air gap between the ridge line and the top plate The differential feeding concept is achieved by etching two slots on the top of the proposed wide RGW to feed the cavity antenna. The proposed antenna achieve a good performance with a 16.5 dBi realized gain, a good symmetrical radiation pattern, and low cross-polarization level (about −35 dB in the E-plane and −27 dB in the H-plane) within 32.5-35.3 GHz frequency range. The proposed structure is simulated, fabricated and measured. The comparison between measured and simulated results shows a good agreement. Thus, this kind of differential feeding showed a promising potential for feeding large cavity antenna arrays used in different MMW applications.

REFERENCES

[1] Z. Pi and F. Khan, "An introduction to millimeter-wave mobile broadband systems," *IEEE Commun. Mag.*, vol. 49, no. 6, pp. 101–107, Jun. 2011.
[2] T. S. Rappaport *et al.*, "Millimeter wave mobile communications for 5G cellular: It will work!" *IEEE Access*, vol. 1, pp. 335–349, May 2013.
[3] T. S. Rappaport, J. N. Murdock, and F. Gutierrez, "State of the art in 60-GHz integrated circuits and systems for wireless communications," *Proc. IEEE*, vol. 99, no. 8, pp. 1390–1436, Aug. 2011.
[4] G. H. Zhai *et al.*, "Folded half mode substrate integrated waveguide 3 dB coupler," *IEEE Microw. Wireless Compon. Lett.*, vol. 18, no. 8, pp. 512–514, Aug. 2008.
[5] B. Sheleg and B. E. Spielman, "Broadband (7–18 GHz) 10 dB overlay coupler for MIC application," *Electron. Lett.*, vol. 11, no. 8, pp. 175–176, Apr. 1975.
[6] A. A. Sakr, W. M. Dyab, and K. Wu, "Theory of polarization-selective coupling and its application to design of planar orthomode transducers," *IEEE Trans. Antennas Propag.*, vol. 66, no. 2, pp. 749–762, Feb. 2017.
[7] A. A. Sakr, W. Dyab, and K. Wu, "Design methodologies of compact orthomode transducers based on mechanism of polarization selectivity," *IEEE Trans. Microw. Theory Techn.*, vol. 66, no. 3, pp. 1279–1290, Mar. 2018.
[8] F. Alessandri, M. Giordano, M. Guglielmi, G. Martirano, and F. Vitulli, "A new multiple-tuned six-port Riblet-type directional coupler in rectangular waveguide," *IEEE Trans. Microw. Theory Techn.*, vol. 51, no. 5, pp. 1441–1448, May 2003.
[9] H. J. Riblet, "The short-slot hybrid junction," *Proc. IRE*, vol. 40, no. 2, pp. 180–184, Feb. 1952.
[10] J. F. Xu, Z. N. Chen, X. M. Qing, and W. Hong, "Bandwidth enhancement for a 60 GHz substrate integrated waveguide fed cavity array antenna on LTCC," *IEEE Trans. Antennas Progag.*, vol. 59, no. 3, pp. 826–832, Mar. 2011.
[11] J. F. Xu, W. Hong, P. Chen, and K. Wu, "Design and implementation of low sidelobe substrate integrated waveguide longitudinal slot array antennas," *IET Microw., Antennas Propag.*, vol. 3, no. 5, pp. 790–797, Jul. 2009.
[12] G. Q. Luo, Z. F. Hu, W. J. Li, X. H. Zhang, L. L. Sun, and J. F. Zheng, "Bandwidth-enhanced low-profile cavity-backed slot antenna by using hybrid SIW cavity modes," *IEEE Trans. Antennas Propag.*, vol. 60, no. 4, pp. 1698–1704, Apr. 2012.
[13] W. Han, F. Yang, J. Ouyang, and P. Yang, "Single-fed high-gain circularly polarized slotted cavity antenna using TE 330 mode," in *Proc. IEEE Int. Symp. Antennas Propag. USNC/URSI Nat. Radio Sci. Meeting*, Jul. 2015, pp. 677–678.
[14] M. Asaadi and A. Sebak, "High-gain low-profile circularly polarized slotted SIW cavity antenna for MMW applications," *IEEE Antennas Wireless Propag. Lett.*, vol. 16, pp. 752–755, 2016.
[15] W. Han, F. Yang, R. Long, L. Zhou, and F. Yan, "Single-fed low-profile high-gain circularly polarized slotted cavity antenna using a high-order mode," *IEEE Antennas Wireless Propag. Lett.*, vol. 15, pp. 110–113, 2016.
[16] H. Jin, K.-S. Chin, W. Che, C.-C. Chang, H.-J. Li, and Q. Xue, "Differential-fed patch antenna arrays with low cross polarization and wide bandwidths," *IEEE Antennas Wireless Propag. Lett.*, vol. 13, pp. 1069–1072, 2014.
[17] Z. Zhu, C. Chen, Y. Chen, G. Xue, and W. Wu, "A single layer low cross-polarization antenna array based on differential-feed," in *Proc. IEEE Int. Workshop Electromagn. Appl. Student Innov. Competition (iWEM)*, May 2016, pp. 1–3.
[18] M. M. M. Ali and A. Sebak, "Compact printed ridge gap waveguide crossover for future 5G wireless communication system," *IEEE Microw. Wireless Compon. Lett.*, vol. 28, no. 7, pp. 549–551, Jul. 2018.
[19] M. H. M. Shamim, H. Attia, M. S. Sharawi, and A. A. Kishk, "60 GHz circularly polarized dielectric resonator antenna fed by printed ridge gap waveguide," in *Proc. IEEE 28th Annu. Int. Symp. Pers., Indoor, Mobile Radio Commun. (PIMRC)*, Oct. 2017, pp. 1–4.
[20] M. S. Sorkherizi, A. Dadgarpour, and A. A. Kishk, "Planar high-efficiency antenna array using new printed ridge gap waveguide technology," *IEEE Trans. Antennas Propag.*, vol. 65, no. 7, pp. 3772–3776, Jul. 2017.
[21] M. S. Sorkherizi and A. A. Kishk, "Fully printed gap waveguide with facilitated design properties," *IEEE Microw. Wireless Compon. Lett.*, vol. 26, no. 9, pp. 657–659, Sep. 2016.
[22] A. Polemi, S. Maci, and P.-S. Kildal, "Dispersion characteristics of a metamaterial-based parallel-plate ridge gap waveguide realized by bed of nails," *IEEE Trans. Antennas Propag.*, vol. 59, no. 3, pp. 904–913, Mar. 2011.
[23] P.-S. Kildal, A. U. Zaman, E. Rajo-Iglesias, E. Alfonso, and A. Valero-Nogueira, "Design and experimental verification of ridge gap waveguide in bed of nails for parallel-plate mode suppression," *IET Microw., Antennas Propag.*, vol. 5, no. 3, pp. 262–270, Mar. 2011.
[24] S. I. Shams and A. A. Kishk, "Design of 3-dB hybrid coupler based on RGW technology," *IEEE Trans. Microw. Theory Techn.*, vol. 65, no. 10, pp. 3849–3855, Oct. 2017.
[25] C. Wu, H. Wang, X. Jiang, S. Quan, and X. Liu, "High-gain dual-polarization higher order mode substrate integrated cavity antenna array," in *Proc. 11th Int. Symp. Antennas, Propag. EM Theory (ISAPE)*, Oct. 2016, pp. 129–131.
[26] T. Mikulasek, J. Lacik, J. Puskely, and Z. Raida, "Design of aperture-coupled microstrip patch antenna array fed by SIW for 60 GHz band," *IET Microw., Antennas Propag.*, vol. 10, no. 3, pp. 288–292, Feb. 2016.
[27] T. Li and W. B. Dou, "Millimetre-wave slotted array antenna based on double-layer substrate integrated waveguide," *IET Microw., Antennas Propag.*, vol. 9, no. 9, pp. 882–888, Jan. 2015.
[28] J. Xu, Z. N. Chen, X. Qing, and W. Hong, "A single-layer SIW slot array antenna with TE_{20} mode," in *Proc. Asia–Pacific Microw. Conf.*, Dec. 2011, pp. 1330–1333.

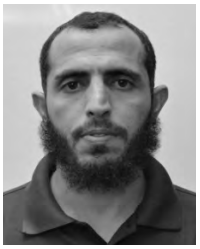

ABDULADEEM BELTAYIB received the B.Sc. degree in electronics and communications engineering and the M.Sc. degree in electrical and computer engineering from the College of Electronic Technology, The Libyan Academy, Bani Walid, Libya, in 2003 and 2007, respectively. He is currently pursuing the Ph.D. degree in electrical and computer engineering with Concordia University, Montréal, QC, Canada. From 2008 to 2013, he was a Lecturer with the Communication Department, Faculty of Engineering, High Institution Electronics Technology, Bani Walid, Libya, where he was a Teaching Assistant with the Department of Communication Engineering. His current research interests include analysis and antenna design, high gain millimeter-wave antennas, and ridge gap wave guide and metamaterial.

ISLAM AFIFI (GS'18) received the B.Sc. degree in electronics and communication engineering and the M.Sc. degree in engineering physics from Cairo University, Cairo, Egypt, in 2009 and 2014, respectively. He is currently pursuing the Ph.D. degree in electrical and computer engineering, Concordia University, Montréal, QC, Canada. His research interests include millimeterwave microwave components and antennas. He was a Teaching and Research Assistant with the Engineering Mathematics and Physics Department, from 2009 to 2014, and a Senior Teaching Assistant, from 2014 to 2016.

ABDEL-RAZIK SEBAK (LF'10) received the B.Sc. degree (Hons.) in electrical engineering from Cairo University, Cairo, Egypt, in 1976, the B.Sc. degree in applied mathematics from Ain Shams University, Cairo, in 1978, and the M.Eng. and Ph.D. degrees in electrical engineering from the University of Manitoba, Winnipeg, MB, Canada, in 1982 and 1984, respectively. From 1984 to 1986, he was with CMC Electronics, where he was involved in the design of microstrip-phased array antennas. From 1987 to 2002, he was a Professor with the Department of Electronics and Communication Engineering, University of Manitoba. He is currently a Professor with the Department of Electrical and Computer Engineering, Concordia University, Montréal, QC, Canada. His research interests include phased-array antennas, millimeter-wave antennas and imaging, computational electromagnetics, and the interaction of EM waves with engineered materials and bio electromagnetics. He is a member of the Canadian National Committee, International Union of Radio Science Commission B. He was a recipient of the 1992 and 2000 University of Manitoba Merit Award for outstanding teaching and research. He has served as the Technical Program Chair for the 2002 IEEE CCECE Conference and the 2006 URSIANTEM Symposium, and the Chair for the IEEE Canada Award and Recognition Committee, from 2002 to 2004. He is the Technical Program Co-Chair of the 2015 IEEE ICUWB Conference.